Rotation Speed Differences of Impurity Species in the DIII-D Tokamak and Comparison with Neoclassical Theory

L.R. Baylor, K.H. Burrell*, R.J. Groebner*, D.R. Ernst# , W.A. Houlberg, M. Murakami, and The *DIII-D Team*

Oak Ridge National Laboratory

***General Atomics,**

#Princeton Plasma Physics Laboratory

at the

43rd Meeting of the APS Division of Plasma Physics

Oct 31, 2001

Long Beach, CA

Abstract

Toroidal rotation velocity profiles of carbon, helium, and neon have been measured on the DIII-D tokamak with the charge exchange recombination (CER) spectroscopy diagnostic. Neoclassical theory predicts a relation between the toroidal rotation speeds of the different impurities. In order to make an accurate comparison with theory, the CER data analysis requires taking into account the energy dependent charge-exchange cross sections for the different species. Upgrades in the CER analysis code to take this cross-section effect into account are being made and checked with transitions that have different energy dependence. The toroidal rotation speed of these impurities was measured in quiescent double-barrier (QDB) mode, RI-mode, and PEP-mode discharges. Differences in the toroidal rotation speeds of the impurities in the same discharge are compared with neoclassical theory using the FORCEBAL/NCLASS and TRV codes.

Rotation of Impurity Species

- E_r derived from radial force balance:

$$E_r(r) = \frac{\nabla P_C(r)}{Z_c\, e\, n_C(r)} + v_{\phi C}\, B_\theta - v_{\theta C}\, B_\phi$$

where T_i, $v_{\phi C}$, $v_{\varphi C}$ are determined by CER

Since E_r is the same for all species,

Measured

$$= \frac{\nabla P_i(r)}{Z_i\, e\, n_i(r)} + v_{\phi i}\, B_\theta - v_{\theta i}\, B_\phi$$

Neoclassical

Therefore,

$$v_{\phi i} = v_{\theta i}\, B_\phi\, B_\theta^{-1} - B_\theta^{-1} \left(\frac{\nabla P_i(r)}{Z_i\, e\, n_i(r)} + E_r \right)$$

- **NCLASS calculates relative parallel flow between species (determined by the parallel friction from Coulomb collisions). This allows neoclassical determination of $v_{\theta i}$.**
- Largest difference in $v_{\phi i}$ will be in plasma with large ∇P_i

Rotation Data Analyzed with FORCEBAL and NCLASS codes

- Raw input data is processed and then fit to profiles with the 4D fitting codes.
- Profile data is then input with equilibrium to FORCEBAL code, which computes radial force balance.
- NCLASS library [Houlberg] is called by FORCEBAL to obtain neoclassical poloidal rotation flux function.
- Local toroidal and poloidal rotation velocities of any species are reconstructed.

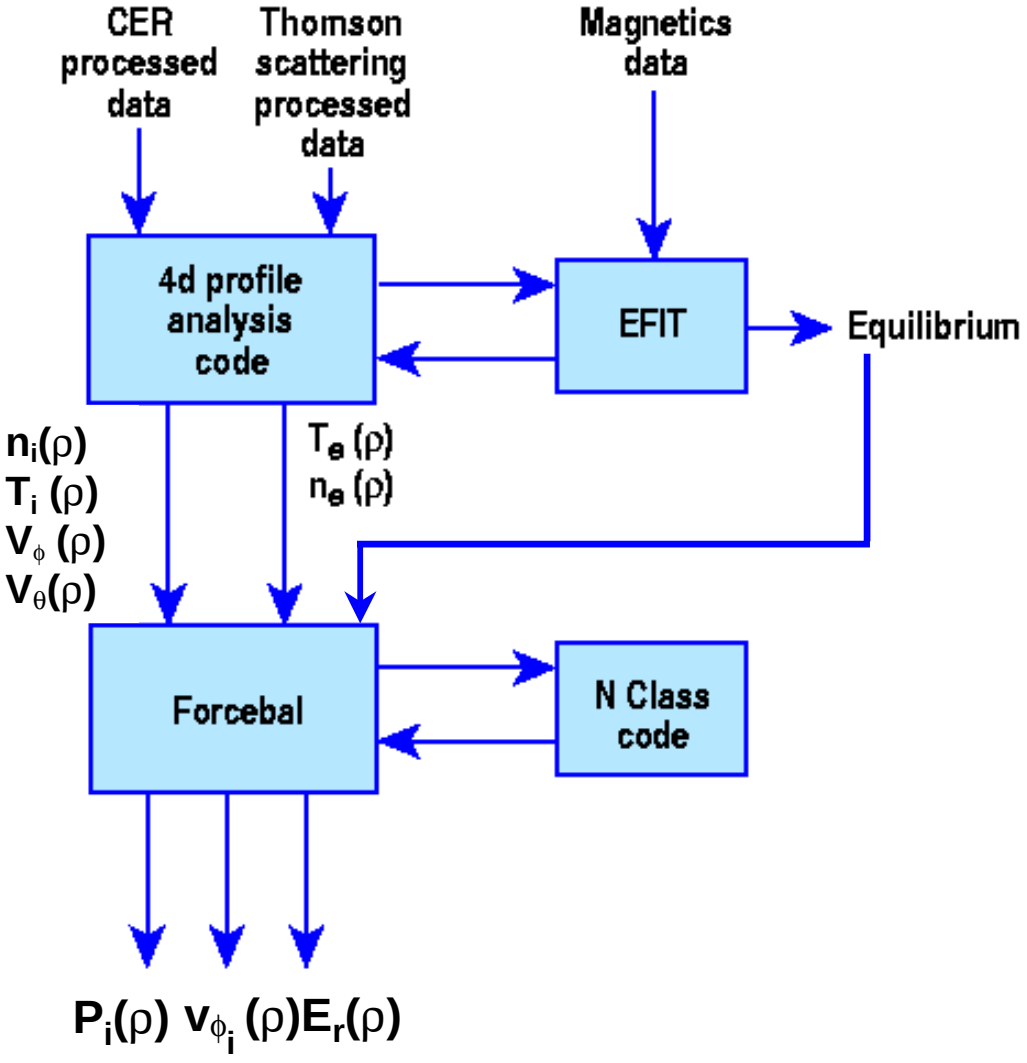

Experimental Plasma Conditions

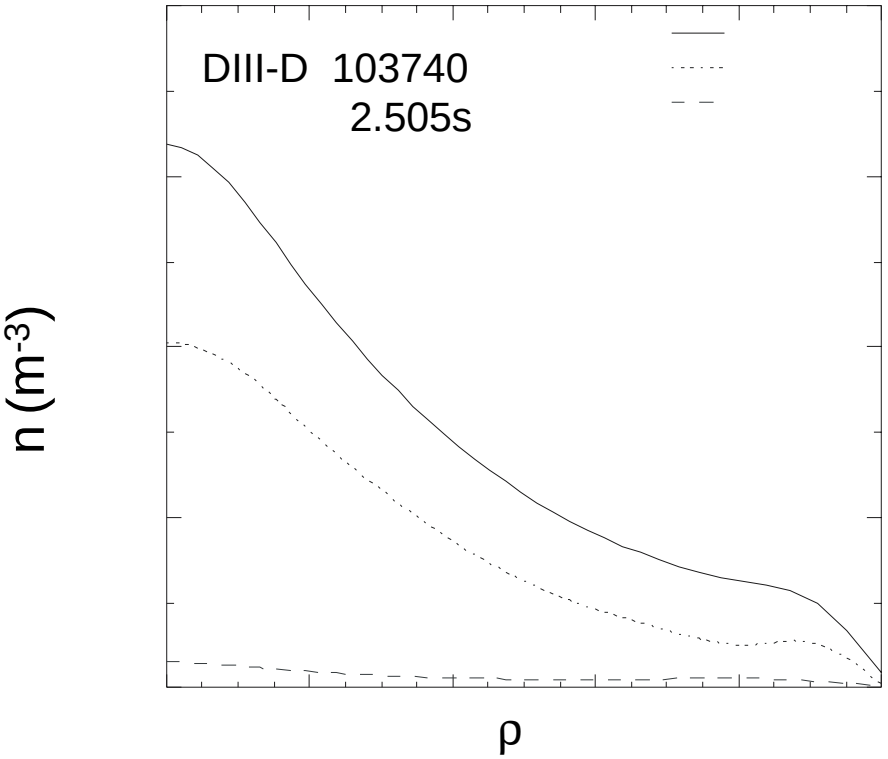

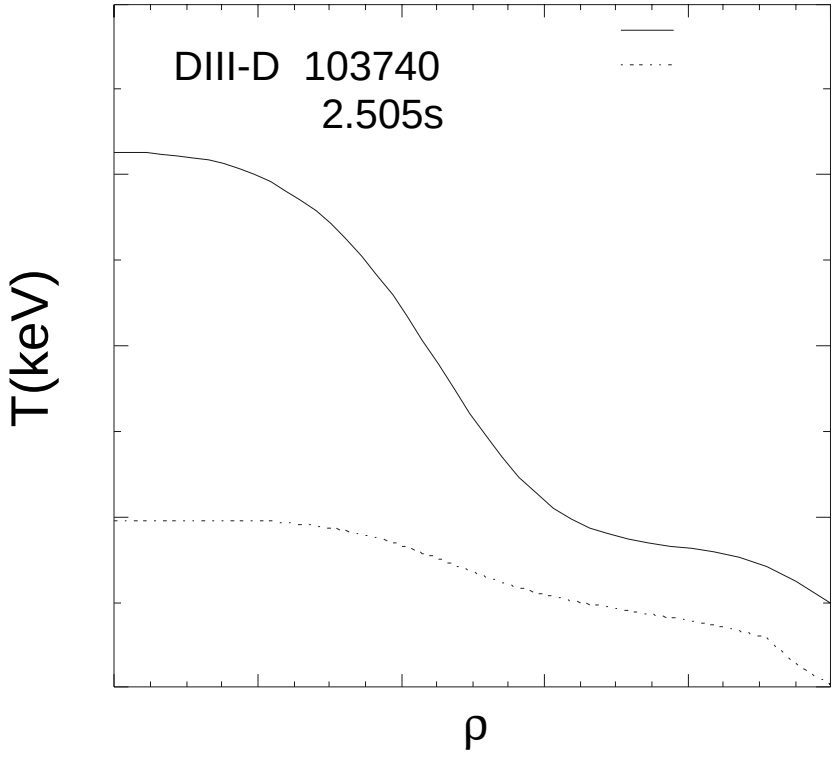

- Quiescent double barrier (QDB) mode plasmas [Burrell] offer the best conditions to observe the difference in toroidal rotation profiles due to the high pressure gradient and low level of anomalous transport.
- These plasmas are characterized with a peaked density profile and broad ITB in the ion channel.

FORCEBAL Predictions for QDB Mode Case

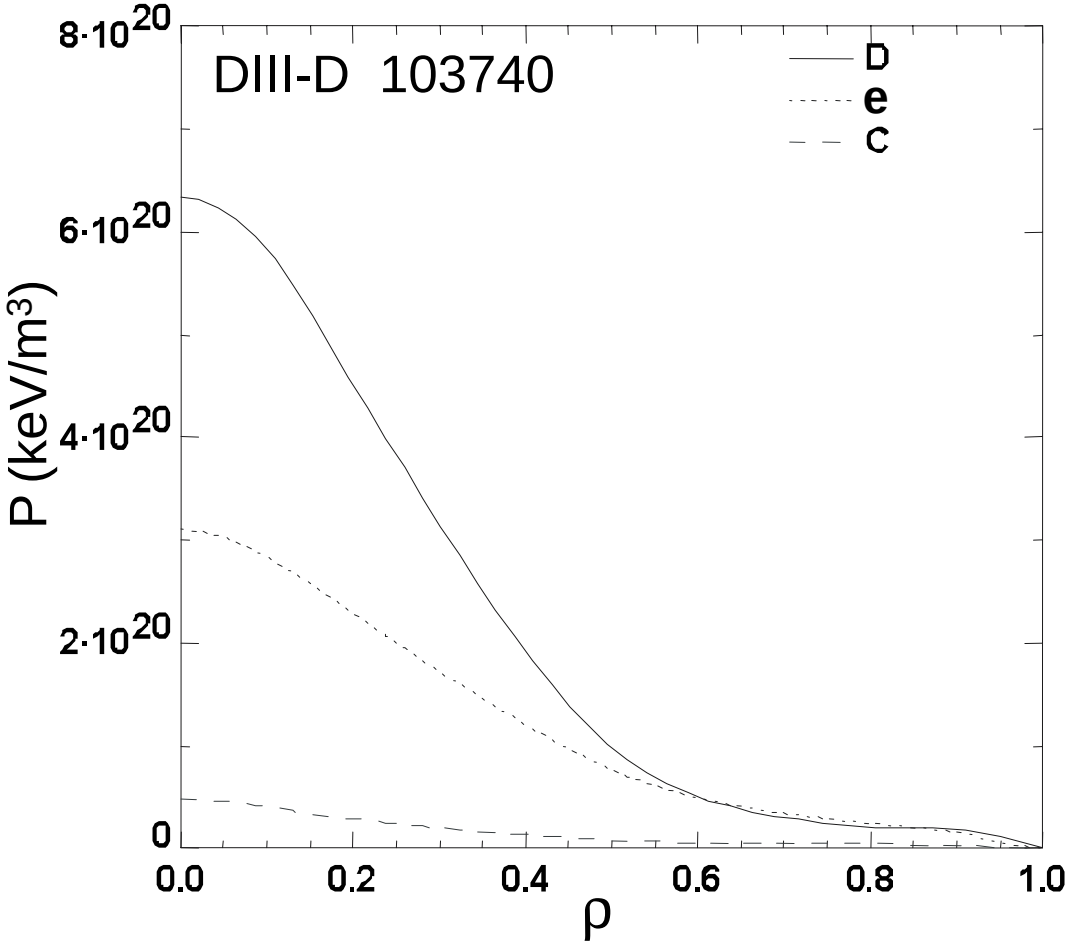

- Pressure profile for D, e, and C from QDB mode case. Strong peaking of the pressure is favorable for the variation in toroidal rotation speeds.

FORCEBAL Radial Electric Field for QDB Mode Case

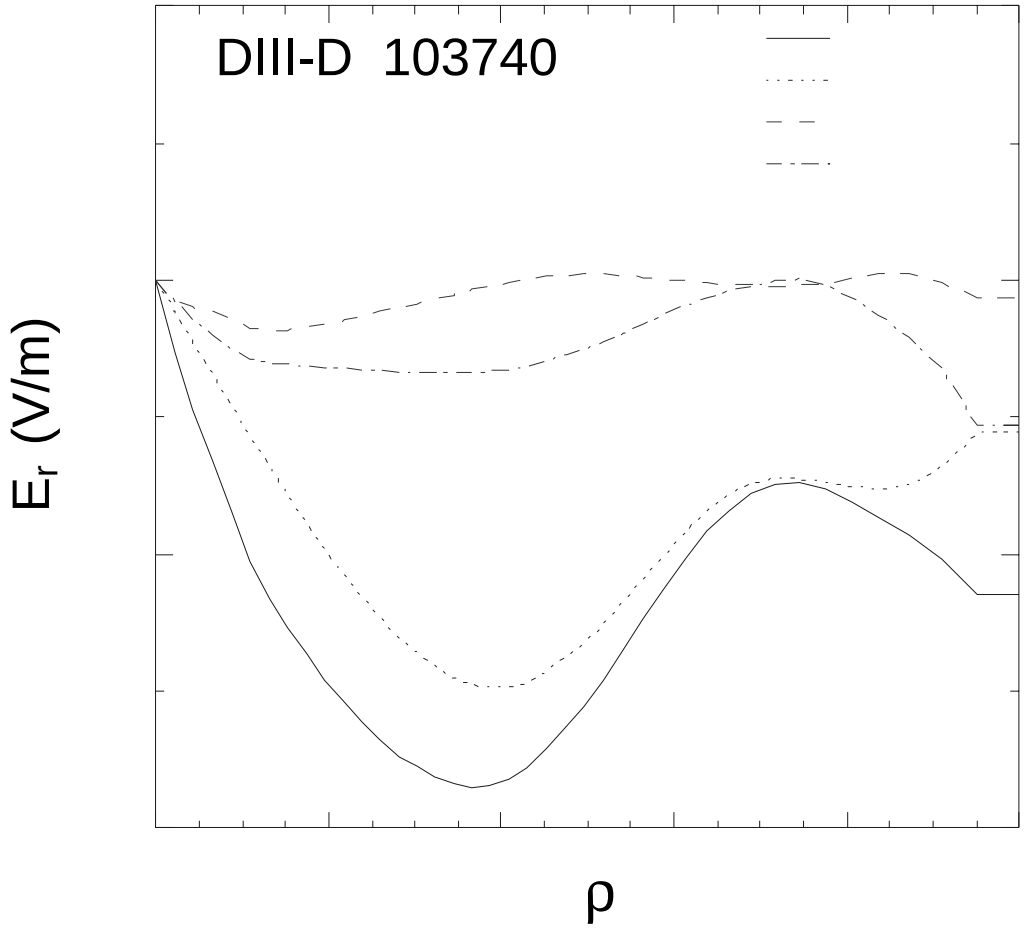

- Radial electric field and components from C profile data.
- The toroidal velocity term is the dominant term.

FORCEBAL V_{tor} Calculations for QDB Mode Case

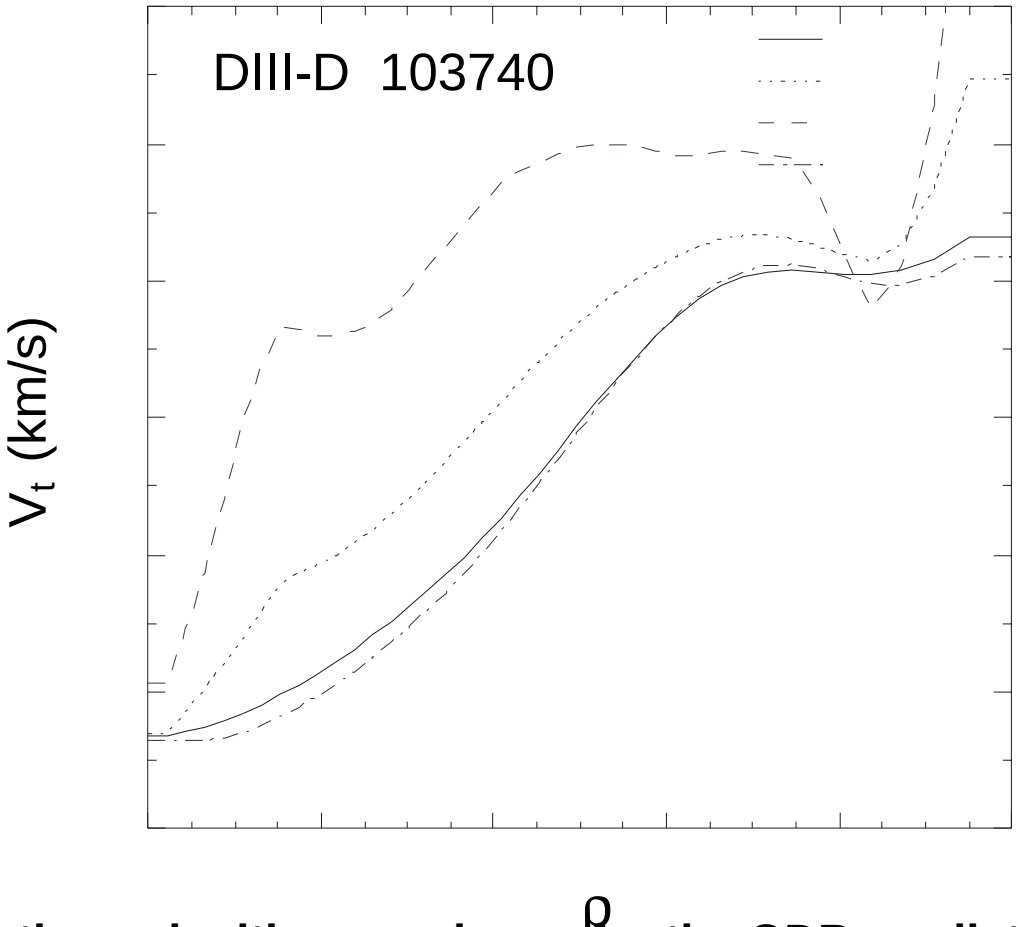

- **Toroidal rotation velocities are shown for the QDB predictive run.Trace amounts of He4 and Ne are assumed with the same density profile shape as the electrons.**
- **C and Ne have similar Vtor, while He4 is expected to be ~100 km/s slower and should be easily measurable. D rotates much slower than the impurity species.**

Predicted Toroidal Mach Numbers for QDB Mode Case

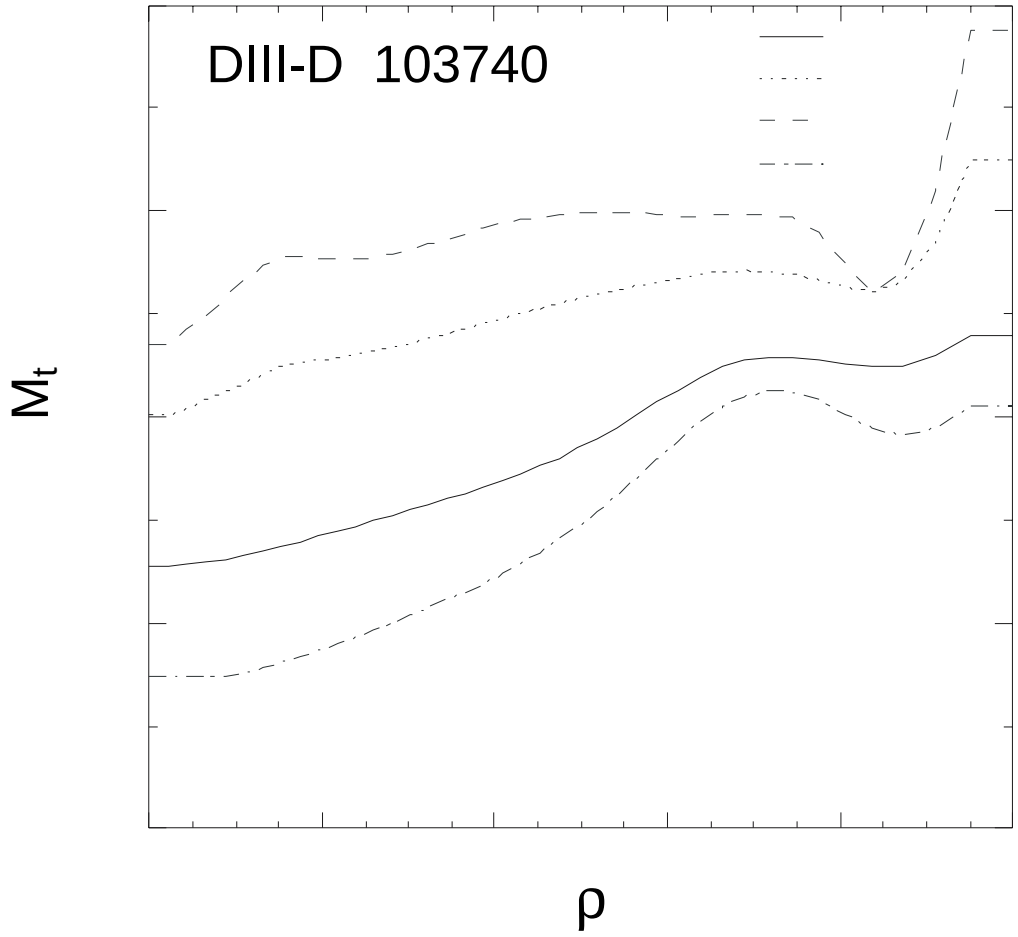

- Toroidal Mach numbers are shown for the QDB predictive run. For C and lighter species the Mach number is < 1 as required for the neoclassical formalism.

Example of Data from Simultaneous C VI, Ne X, and He II Measurements with CER

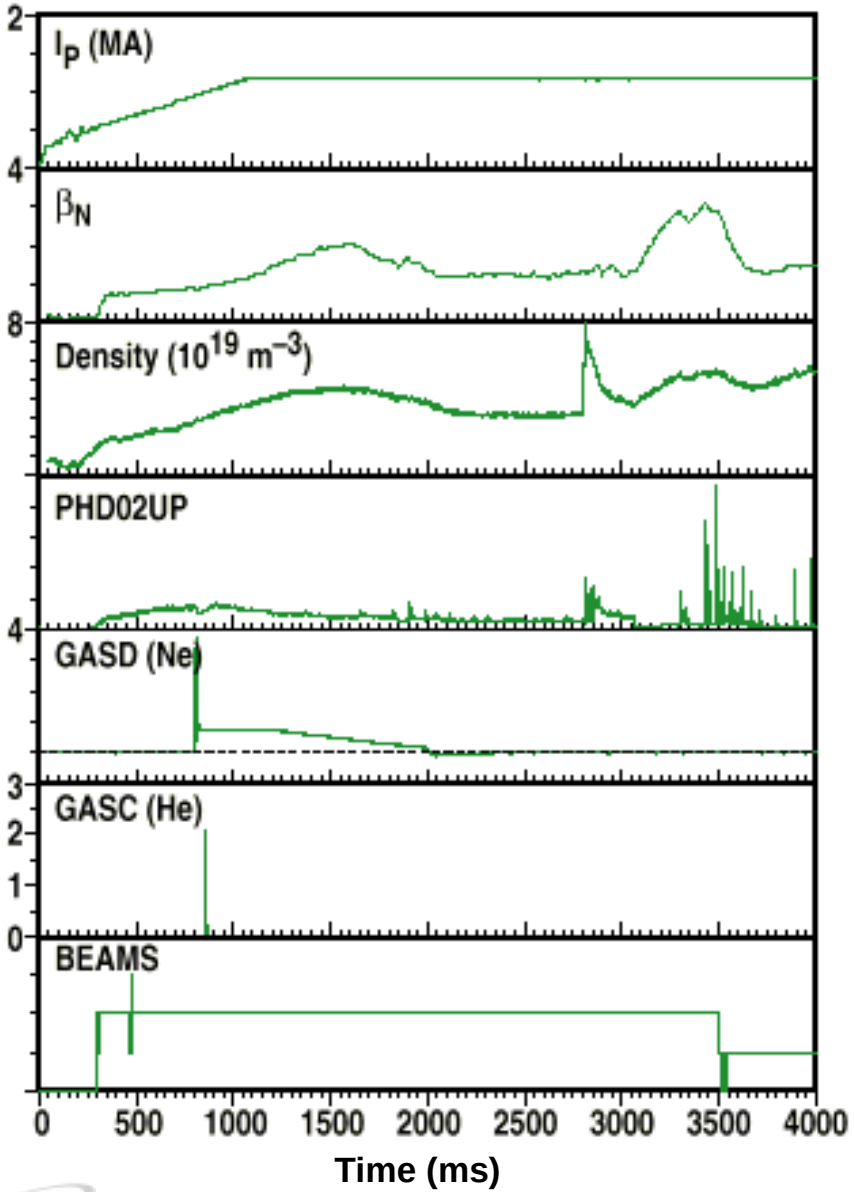

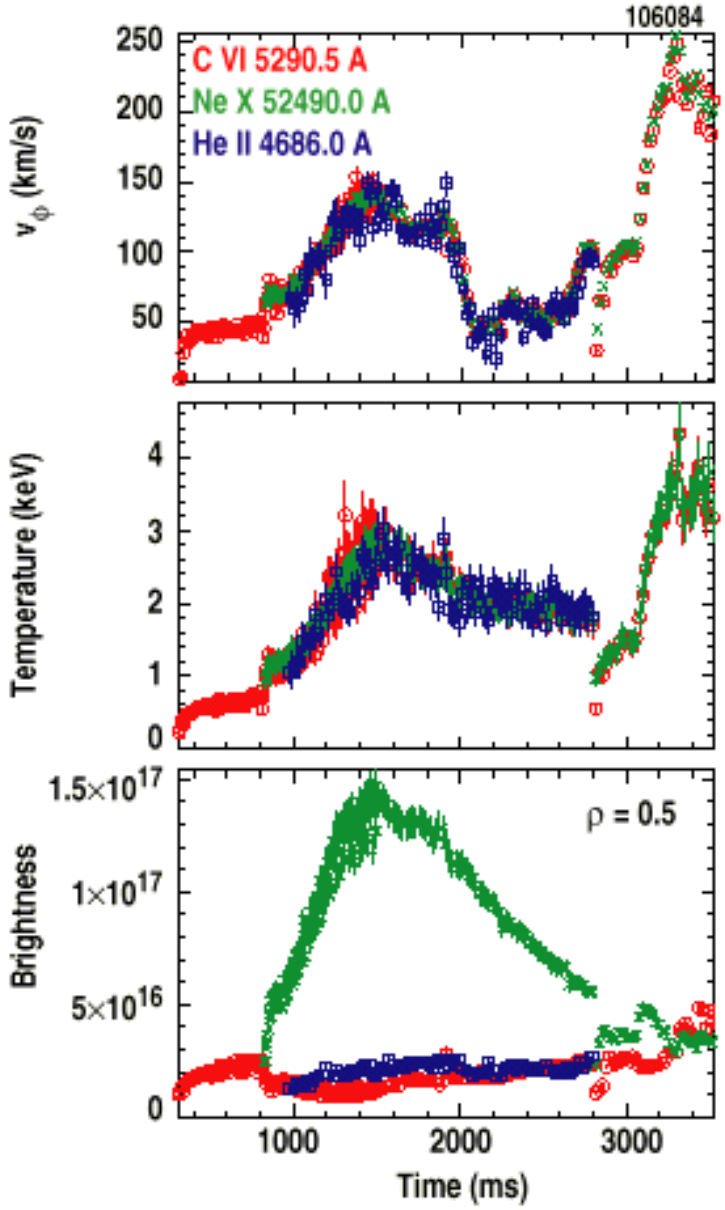

Assessment of Experiment

- Good data sets were obtained in a dedicated experiment in Neon seeded ITB, PEP, and QDB mode plasmas.
- Proper comparison with theory requires analyzing CER data for effects of an energy-dependent charge exchange cross section.
- *Data on previous slide is **not** corrected for the energy-dependent cross section.* The analyzed T_i is not expected to change very much at these conditions (see details below).
- Work to implement the fitting of the CER data with an energy-dependent charge exchange cross section has begun and is being included into the CERFIT spectral fitting software.
- Results using the extended CERFIT program should be available in a few months.

Further Detailed Analysis of CER Data is Needed to Take into Account the Energy Dependent Cross Section

- The charge exchange recombination (CER) diagnostic uses a spectrometer to measure the spectra of charge exchange lines. [Isler]
- The layout of this diagnostic on DIII-D is shown on the following page. [Gohil]
- The Doppler broadened and Doppler shifted visible emission from the relevant ion species (C, He, Ne) is used to determine the ion temperature, T_i, and toroidal v_ϕ, and poloidal v_θ, rotation velocities.
- Comparisons of rotation of main ions and impurity ions were made in the edge [Kim, 1994] where the energy dependent cross-section effects are not so apparent.

CER is Key Diagnostic for these Measurements is CER Layout on DIII-D - Plan View

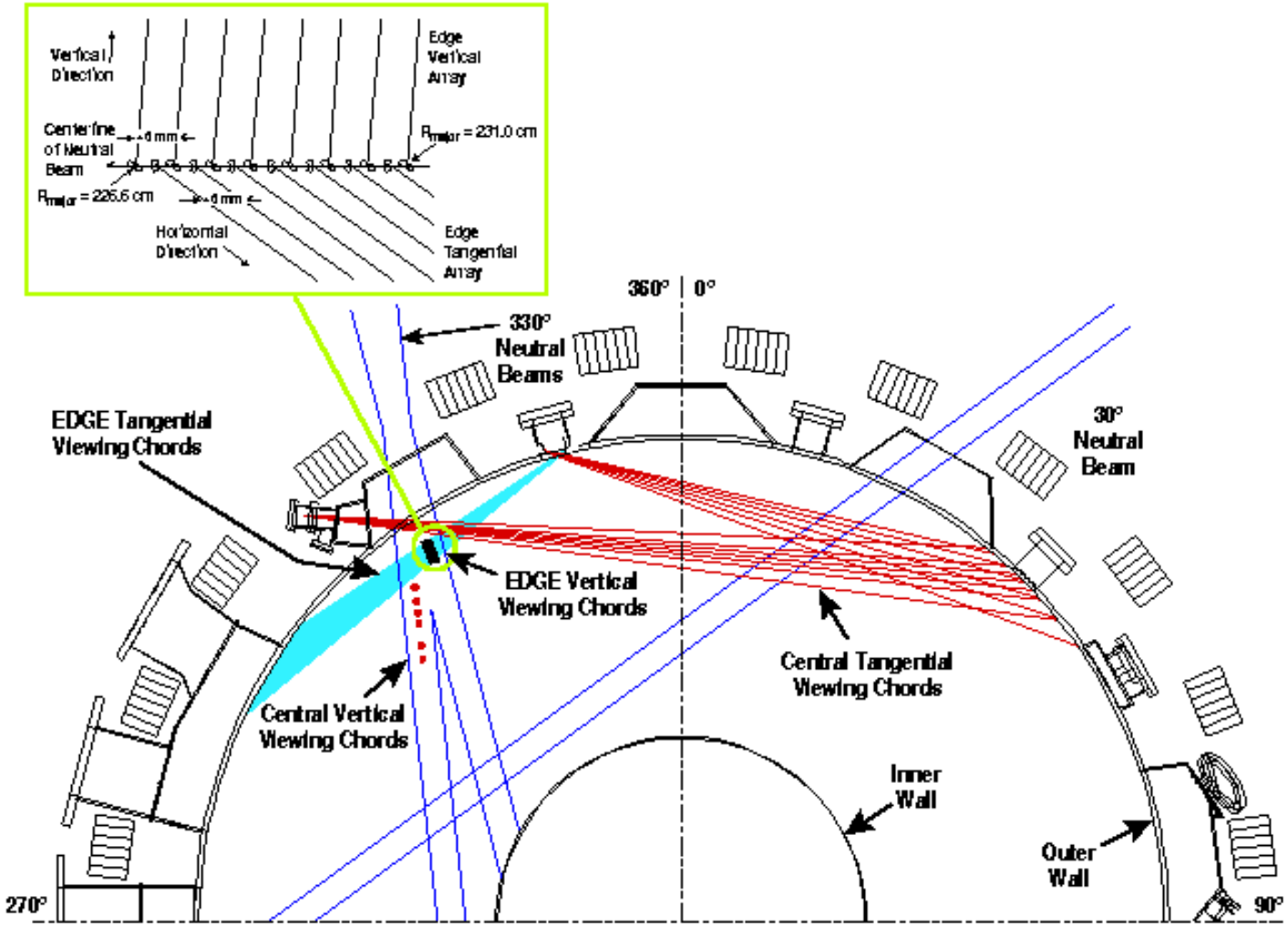

- For further details of the DIII-D CER diagnostic see the web site:
  http://fusion.gat.com/diag/cer

Charge Exchange Process

$$D^0 + A^{+z} \rightarrow D^+ + A^{+(z-1)}$$

beam neutral	impurity ion	impurity ion

The specific emission lines used on DIII-D are:

C^{5+} ($n = 8 \rightarrow 7$), 5291 Å

He^{1+} ($n = 4 \rightarrow 3$), 4685 Å

Ne^{9+} ($n = 11 \rightarrow 10$), 5249 Å

For thermal particles, the Doppler broadening of the observed spectrum represents the local ion temperature and the peak position is a measure of the bulk velocity.

Charge Exchange Emission

The observed charge exchange spectrum is given by:

$$f(v_z) = \int d^3\vec{v}'\, \mathrm{Q}(|\vec{v}' - \vec{v}_b|)\, \delta(v_z' - v_z)\, \frac{1}{\pi^{3/2} v_{th}{}^3} e^{\left[\frac{-(\vec{v}' - \vec{V}_{rot})^2}{v_{th}{}^2}\right]}$$

where $\mathrm{Q}(|v|) = \sigma_{cx}(|v|)\, v$ is the emission rate with the energy-dependent cross section σ_{cx}. $\boldsymbol{V_{rot}}$ is the rotational velocity vector of the plasma. $\boldsymbol{V_b}$ is the velocity vector of the beam neutrals.

- The line of sight is assumed to be along the z axis and the distribution function is assumed to be a thermal (Maxwellian) distribution function.
- The emission rates Q for the species of interest including the energy-dependent cross section are shown in the following slide.

Energy Dependent Cross Sections

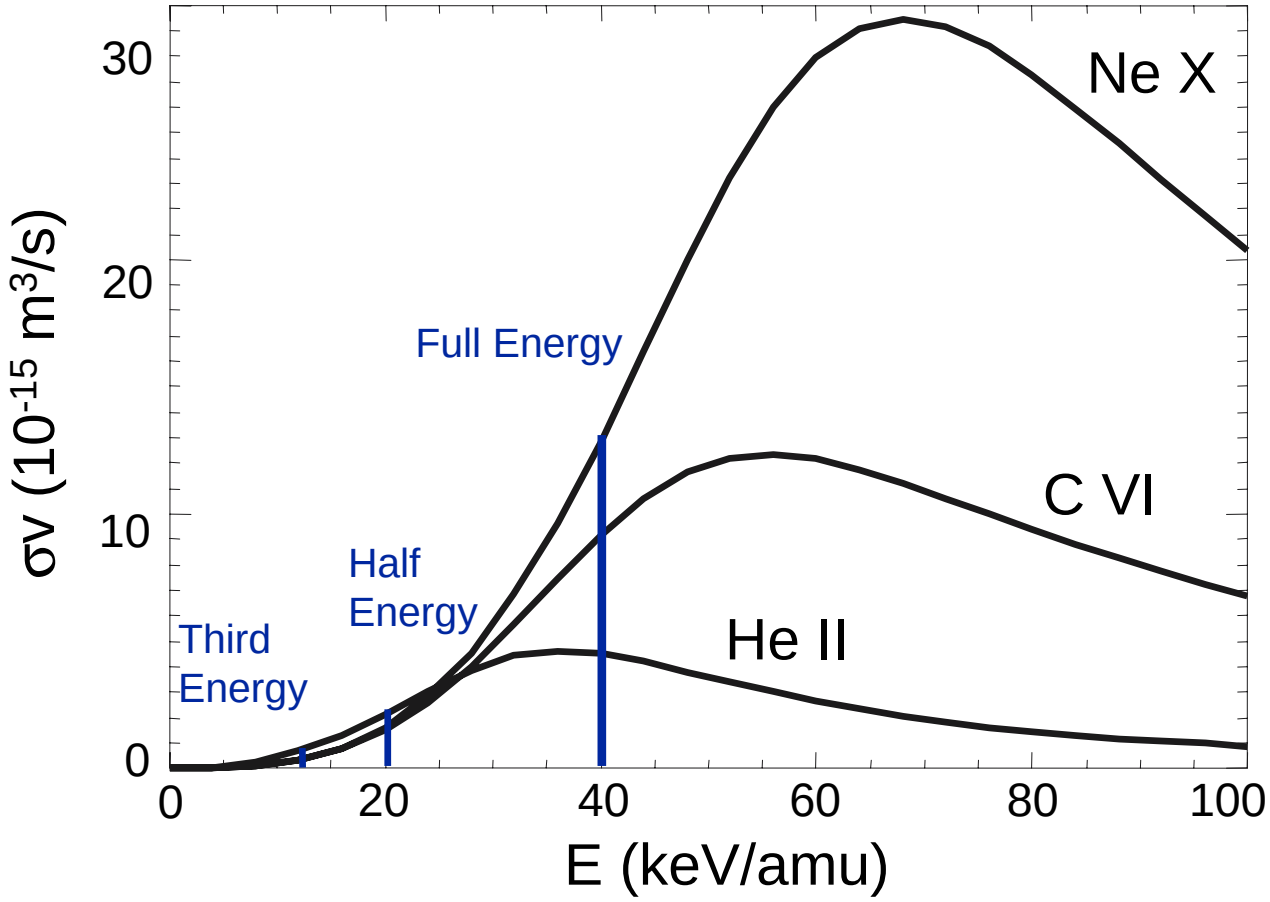

- The three beam energy components sample an energy dependent cross section.
- An analytical approximation of the cross section [von Hellermann] is used.

Beam Attenuation Calculation Used to Determine Beam Species Mix

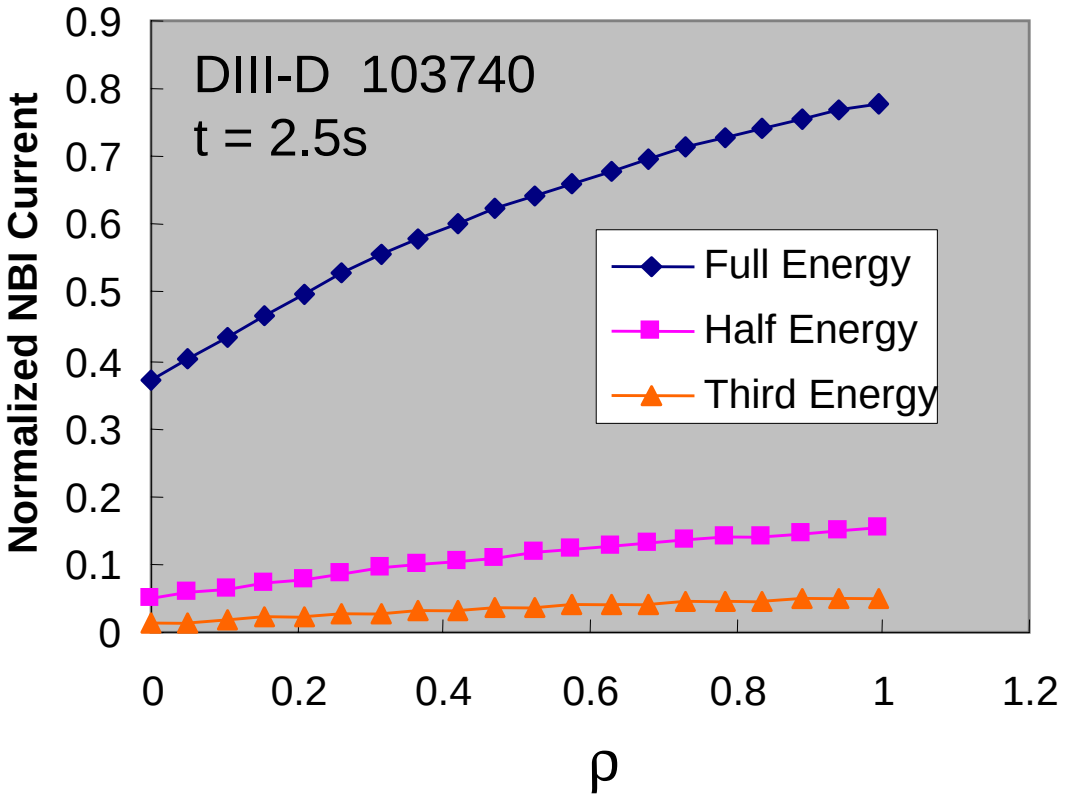

- The shifted CER line results from the three energy components whose relative magnitudes are shown as a function of radius for a QDB plasma.
- Beam attenuation calculation from M. Wade – normalized to 1.0 at the plasma edge.

CER Shifted Line Profile from Energy Dependent Cross Section

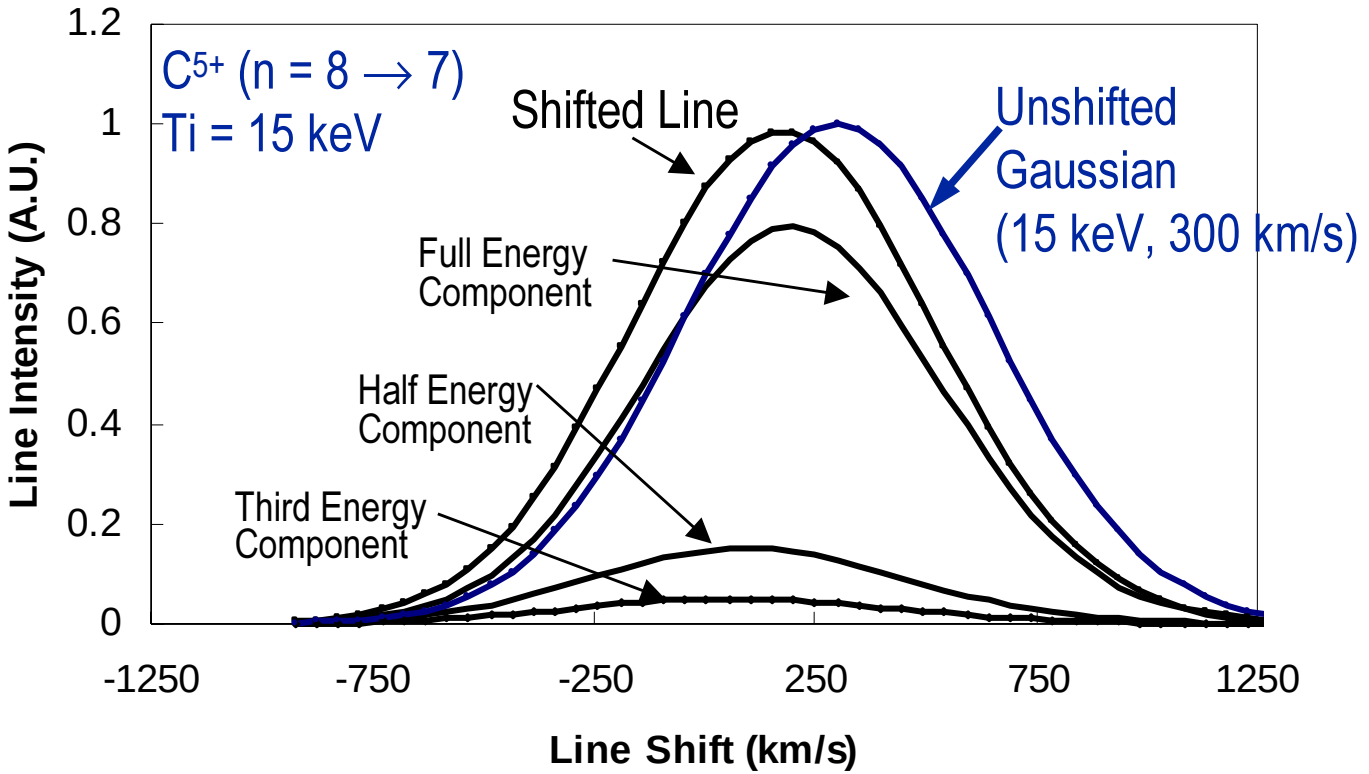

- In this DIII-D QDB example for ρ=0.3, a line shift of ~100 km/s occurs due to the CX cross section. (CXRS code [Groebner], cross section approximation [von Hellermann])
- The shifted line results from the three energy components is very nearly Gaussian in shape.

Variation of Apparent Ti and Vt As a Function of Real Ti

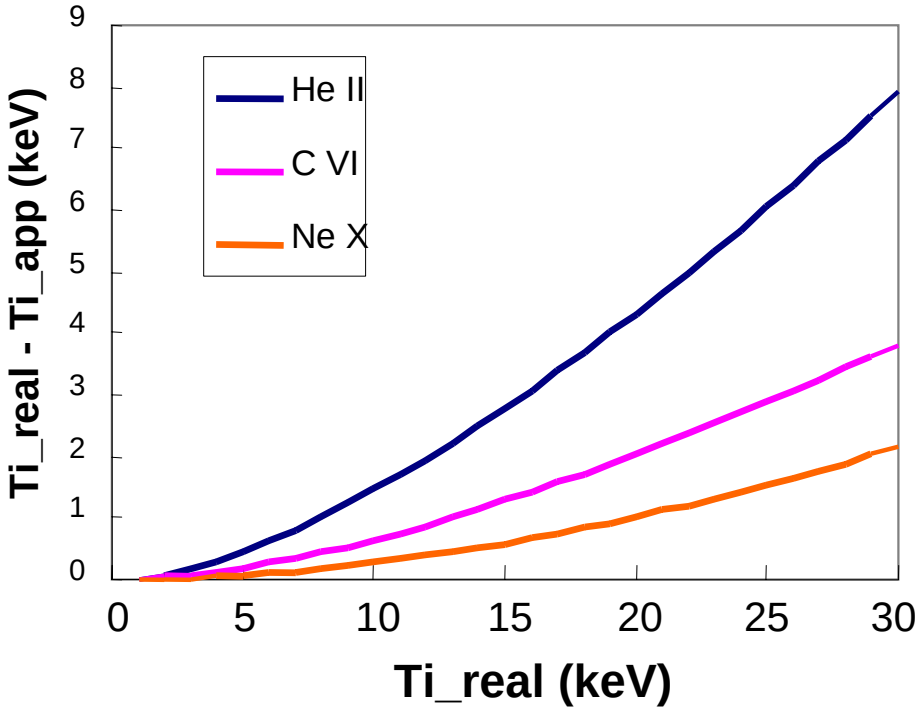

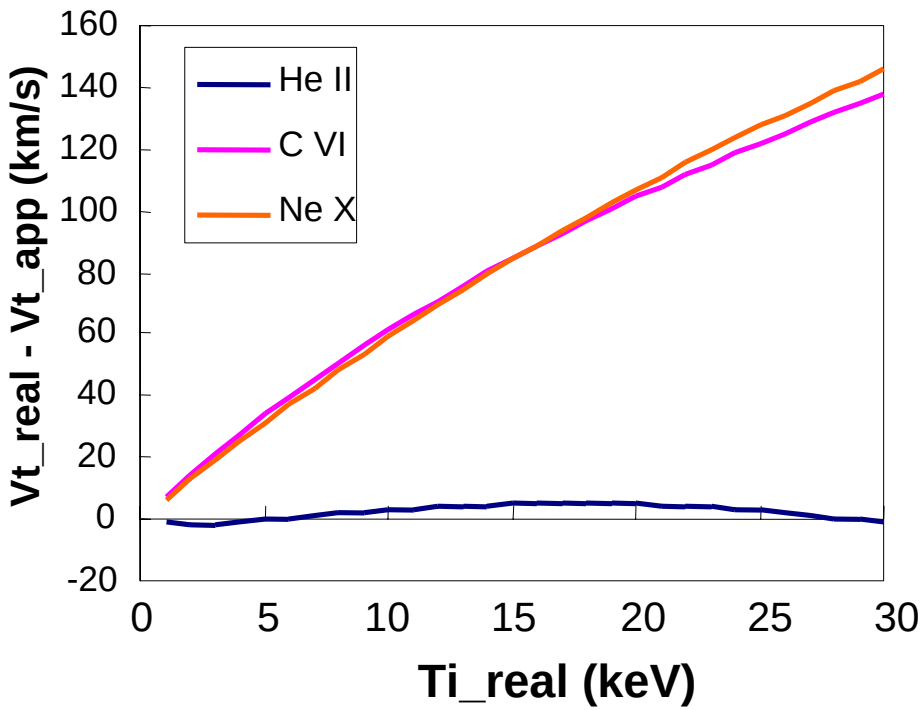

- The apparent Ti and V_t are calculated for a real range of Ti and V_t of 0 km/s at a 45 degree viewing angle. The difference between the real Ti and V_t and the apparent value are found by fitting a Gaussian to the resulting calculated spectrum. Three beam energy values are used.
- The Ti variation is several keV and Vt is ~ 100 km/s for the range of interest in the ITB plasmas.

Variation of Apparent Ti and Vt As a Function of Real Vt

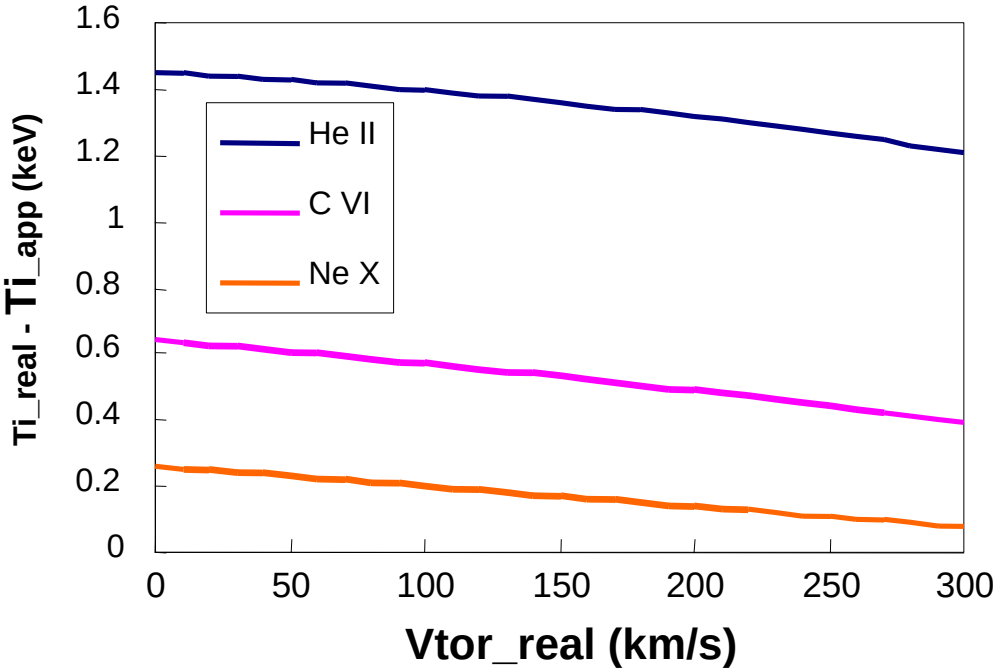

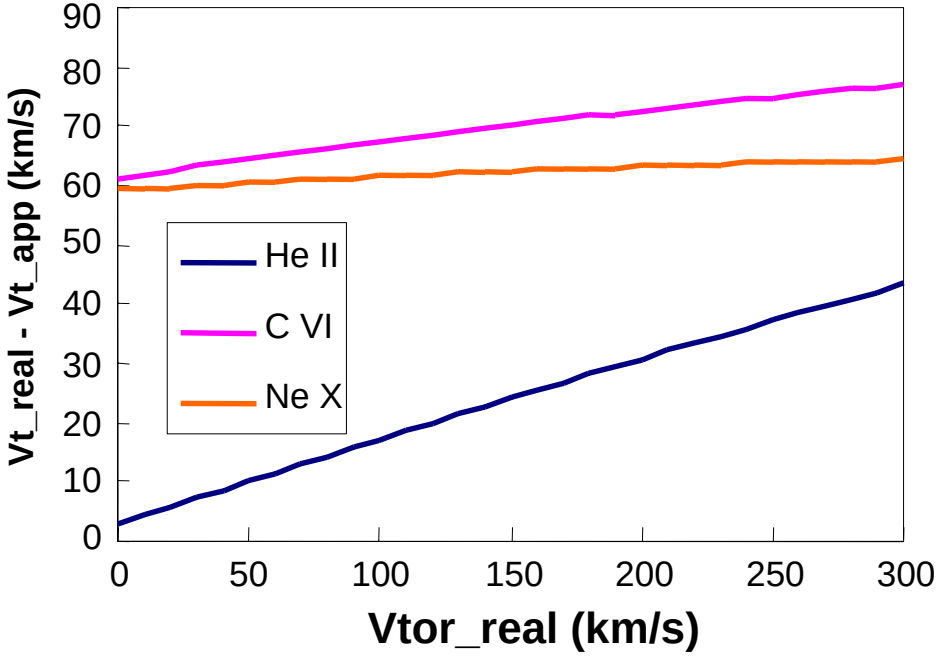

- The apparent Ti and V_t are calculated for a real range of V_t and Ti of 10 keV at a 45 degree viewing angle. The difference between the real Ti and V_t and the apparent value are found by fitting a Gaussian to the resulting calculated spectrum. Three beam energy values are used.
- The V_t variation can be significant for the range of interest in the ITB plasmas.

Convolution with Instrument Function

- The instrument response is fit as a sum of Gaussians of width w. The spectrometer produces a convolution of the line shape with the instrument response, which gives an integral like:

$$h(v_z) = \int_{-\infty}^{\infty} dv_z' \frac{1}{\pi^{1/2} w} e^{\left[\frac{-(v_z - v_z')^2}{w^2}\right]} f(v_z')$$

- The full convolution integral has been implemented and requires 2-5 sec of CPU time on an Alpha 4000 5/300 workstation.
- An efficient and accurate approximation to the full convolution integral can be made by keeping Q constant when doing the v'_z integral [Burrell]. Comparisons of the full integral and approximation are shown on the next page.

Comparison of Convolution and Approximation

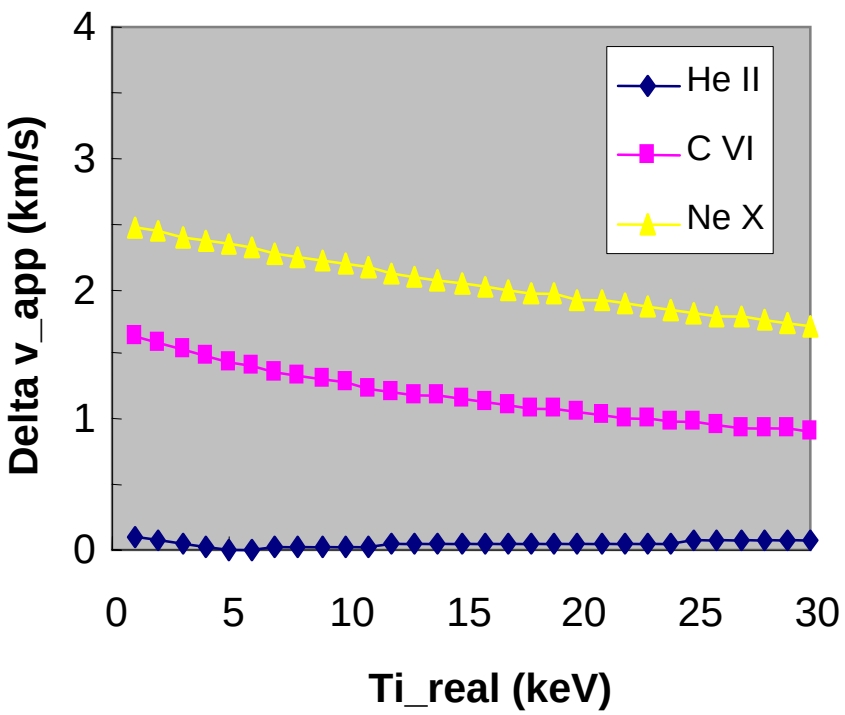

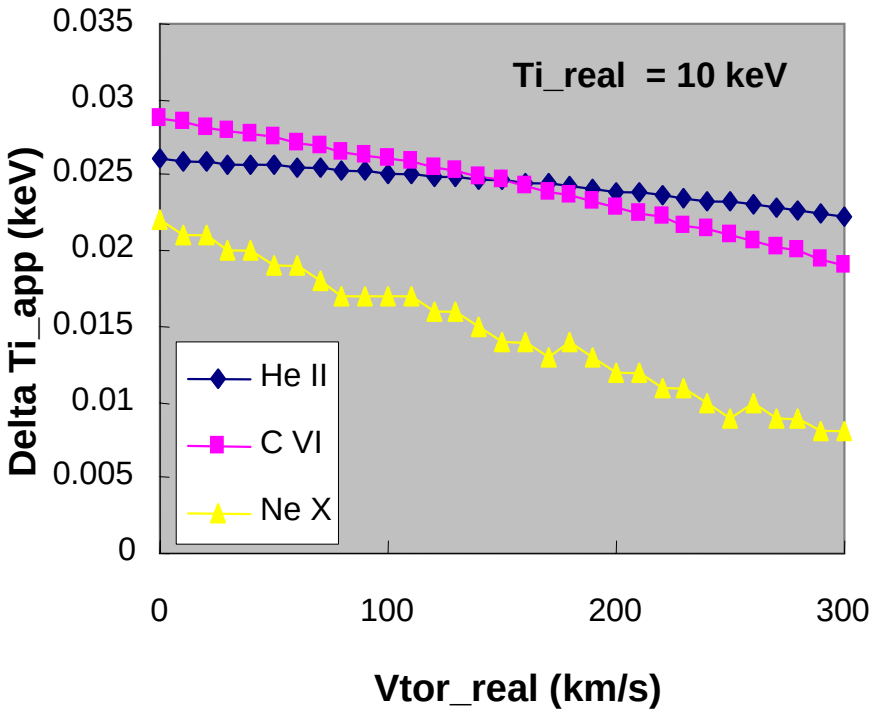

- Comparing the apparent velocity and temperature of the fully convoluted spectra, $h(v_z)$, with the approximation to the full convolution integration shows minimal differences.

Summary

- Experiments have been performed on DIII-D to examine the relationship of the toroidal rotation velocity between different impurity ion species.
- Data has been taken for C VI, He II, and Ne X lines in QDB, PEP, and RI-mode ITB plasmas.
- Initial analysis without taking into account the energy-dependent cross sections is inconclusive.
- Work has been undertaken to implement the energy dependent cross section into the CERFIT spectral fitting code. Benchmarks indicate reasonable CPU time to generate convolved spectra.
- Stay tuned for future detailed analyzed results from these experiments.

References

- **Von Hellerman, M.,** Plasma Phys. Control. Fusion **37** (1995) 71.
- **Burrell,** K.H., Excitation Rate Integral derivation, Unpublished 1998.
- **Houlberg, W.A., et al., NCLASS,** Phys. Plasmas, **4** (1997) 3230.
- **Burrell, K. – Quiescent Double Barrier Mode Paper,** Phys. Plasmas, **8** (2001) 2153.
- **Isler, R.C.,** CER review paper, Plasma Phys. Control. Fusion, **36** (1994) 171.
- **Groebner, R. , CXRS code development,** Unpublished 1999.
- **Gohil, P., et al., The CER Diagnostic System on the DIII-D Tokamak,** Proceedings of 14th Symposium, IEEE (1991) 1199.
- **Bell, R.E., et al.,** TTF 1999.
- **Ernst, D.P., et al.,** Phys. Plasmas, **7** (2000) 615.
- **Kim, J., et al.,** Phys. Rev. Lett. **72**, (1994) 2199.